NANO LETTERS

2009
Vol. 9, No. 1
102-106

# Direct Imaging of Rotational Stacking Faults in Few Layer Graphene

**Jamie H. Warner,*,† Mark H. Rümmeli,‡ Thomas Gemming,‡ Bernd Büchner,‡ and G. Andrew D. Briggs†**

*Department of Materials, Quantum Information Processing Interdisciplinary Research Collaboration, University of Oxford, Parks Road, Oxford, OX1 3PH, United Kingdom, and IFW Dresden, P.O. Box 270116, D-01171 Dresden, Germany*

*Received August 26, 2008; Revised Manuscript Received November 6, 2008*

**ABSTRACT**

**Few layer graphene nanostructures are directly imaged using aberration corrected high-resolution transmission electron microscopy with an electron accelerating voltage of 80 kV. We observe rotational stacking faults in the HRTEM images of 2−6 layers of graphene sheets, giving rise to Moiré patterns. By filtering in the frequency domain using a Fourier transform, we reconstruct the graphene lattice of each sheet and determine the packing structure and relative orientations of up to six separate sets. Direct evidence is obtained for few layer graphene sheets with packing that is different to the standard AB Bernal packing of bulk graphite. This has implications toward bilayer and few layer graphene electronic devices and the determination of their intrinsic structure.**

The interest in graphene has developed rapidly since the first report of its excellent electronic transport properties with electric field effects[1] and a 2D gas of massless Dirac Fermions.[2] Studies on the electronic transport studies of bilayer graphene have shown suppression of the 1/*f* noise compared to monolayer graphene associated with the different band structure.[3] The introduction of rotational stacking faults in AB Bernal stacked graphene bilayers changes the dispersion relationship close to the K-point from parabolic (AB) to linear band behavior (rotation stacking fault) and leads to some monolayer graphene properties being observed in bilayer and multilayer graphene films.[4–6] Techniques to characterize the atomic structure of few layer graphene sheets are critical for its future development in electronic devices.

Scanning tunnelling microscopy is effective at probing the structure of graphite and graphene, along with rotational stacking faults that give rise to superstructure in the STM images. The superstructure is attributed to Moiré patterns derived from complex three-dimensional tunnelling.[8–10] However, STM measurements are experimentally challenging with ultrahigh vacuum (UHV) conditions that make the turn around time for characterization relatively long. Transmission electron microscopy offers a faster approach for directly imaging the atomic structure of rotational stacking faults in few layer graphene, which give rise to Moiré patterns.[11] To date, this has been limited to small rotational stacking faults of 1−10° that result in Moiré patterns with structure greater than a nanometer.[11]

The sp2 bonding of carbon in graphene has a low knock-on threshold for atomic displacement by high energy electrons and this limits the accelerating voltage that can be used in high resolution electron microscopy without inducing significant damage.[12] Prior to the development of low-voltage aberration correction, the resolution of HRTEM at electron accelerating voltages between 80−120 kV was poor in comparison to STM measurements and the atomic structure of graphene could not be well resolved. This has limited the in-depth analysis of the atomic scale structure of few layer graphene using direct imaging with HRTEM.

Recent reports have demonstrated that low-voltage aberration-corrected HRTEM is capable of resolving the full C−C hexagonal structure in monolayer graphene[13,14] and in single-walled carbon nanotubes[14,15] and double-walled carbon nanotubes.[16] It as also been used to image the atomic structure of fullerenes and endohedral fullerenes inside SWNTs.[17] The high-resolution now capable in low-voltage aberration-corrected TEM enables direct characterization of the chirality of graphene structures and the presence of defects without inducing large amounts of structural damage.[13–16]

Here, we use low-voltage aberration corrected HRTEM with an electron accelerating voltage of 80 kV to examine the packing structure of few layer graphene by directly imaging the atomic structure. Rotational stacking faults in the AB Bernal structure of few layer graphene are observed and lead to Moiré patterns. By examining few layer graphene

* To whom correspondence should be addressed. E-mail: Jamie.warner@materials.ox.ac.uk.
† University of Oxford.
‡ IFW Dresden.

10.1021/nl8025949 CCC: $40.75 
**Published on Web 12/15/2008**

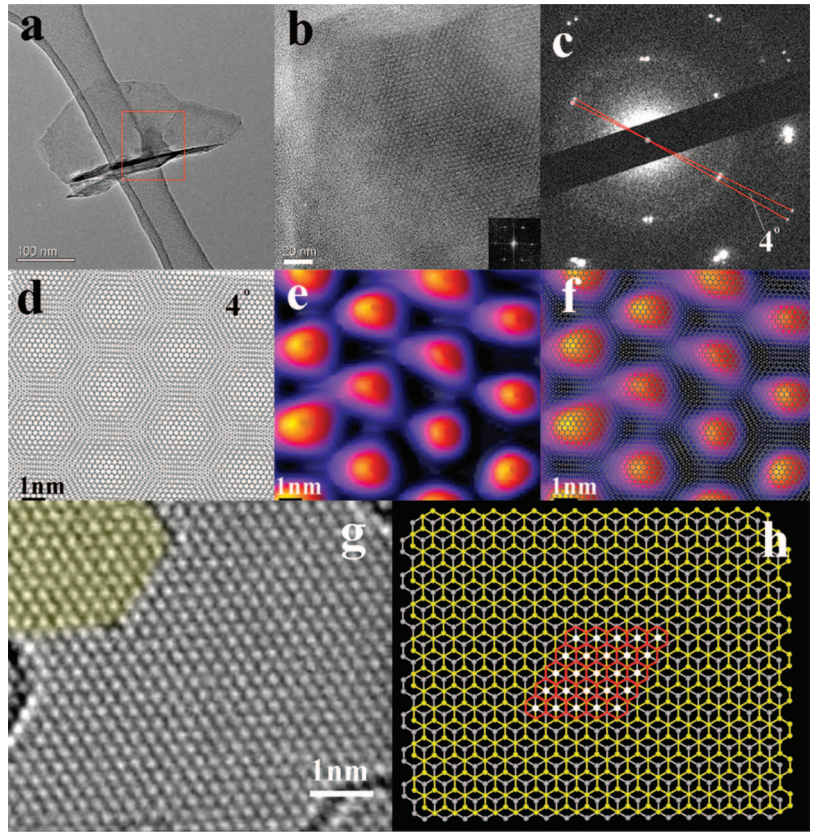


**Figure 1.** (a) TEM image of a few layer graphene nanosheet. (b) HRTEM image of a region with a top layer folded back onto itself giving rise to Moiré pattern. (c) Selected area electron diffraction pattern from the region indicated with a red box in panel a. (d) Structural representation of two graphene sheets with 4° rotation, giving rise to a Moiré pattern. (e) HRTEM image of Moire pattern from panel b in false color to enhance contrast. (f) Overlay of color HRTEM image in panel e with Moire pattern generated in panel d. (g) HRTEM image of few layer graphene with AB Bernal stacking with no Moire patterns (h) Structural representation of two graphene layers with AB Bernal stacking, with white spots indicated regions of overlapping C atoms and red hexagons indicating the structure observed in the HRTEM image of panel g.

nanosheets at the edges we found layers ranged between 1−6. The HRTEM images are examined in the frequency domain, filtered, and an image of each graphene sheet is reconstructed. This enabled rotational stacking faults with up to 6 different orientations to be determined.

Few layer graphene nanosheets were prepared by ultrasonicating graphite in 1,2-dichloroethane for 30 min to form a suspension. This suspension was then centrifuged at 5000 rpm for 5 min to remove large aggregates. This leaves a clear light brown supernatant solution with no sign of aggregates. TEM samples were prepared by dipping a lacey carbon-coated TEM grid into the solution and allowing to dry. This resulted in graphene nanosheets typically between 1−6 layers thick and 100−500 nm in diameter. HRTEM was performed on a FEI Titan HRTEM operating at 80 kV with third order spherical aberration correction to directly image the C−C hexagonal graphene structure. TEM of graphene nanosheets and selected area electron diffraction were performed using a JEOL 4000 operating at 80 kV with a $LaB_6$ filament. Image simulations of bilayer graphene were performed using JEMS computer software.

HRTEM examination of graphene sheets with a relative rotation between them shows the presence of Moiré patterns. A small angle between 1−10° produces patterns with periodic spacing in the nanometer range. Figure 1a shows a TEM image of a small few layer graphene nanosheet containing a top layer that has folded back upon itself, indicated with a red box. This resulted in the Moiré pattern imaged in Figure 1b with a hexagonal structure. The TEM images in Figure 1a,b were obtained without aberration correction using the JEOL 4000. A fast Fourier transform (FFT) of Figure 1b is included in the inset and shows six spots for the hexagonal pattern with a measured periodicity of 3.3 nm. To examine the relative angles between the graphene layers, selected area electron diffraction (SAED) was taken for the region observed in Figure 1b. The SAED in Figure 1c shows two sets of hexagonal spots in the diffraction pattern with a measure angle of 4° between them. Figure 1d shows the structural representation of two graphene sheets with 4° relative rotation and the Moiré pattern generated shows a hexagonal pattern with periodicity close to 3.3 nm. Figure 1e shows a portion of the HRTEM in Figure 1b presented in color for enhanced contrast, and in Figure 1f the Moiré pattern is overlaid with the colored TEM image. An excellent correlation is observed and confirms the Moiré pattern is due to a rotation of 4° between graphene layers. Further advancements beyond the images presented in Figure 1a−f require the use of aberration corrected low-voltage HRTEM in order to resolve the C−C bonds and the

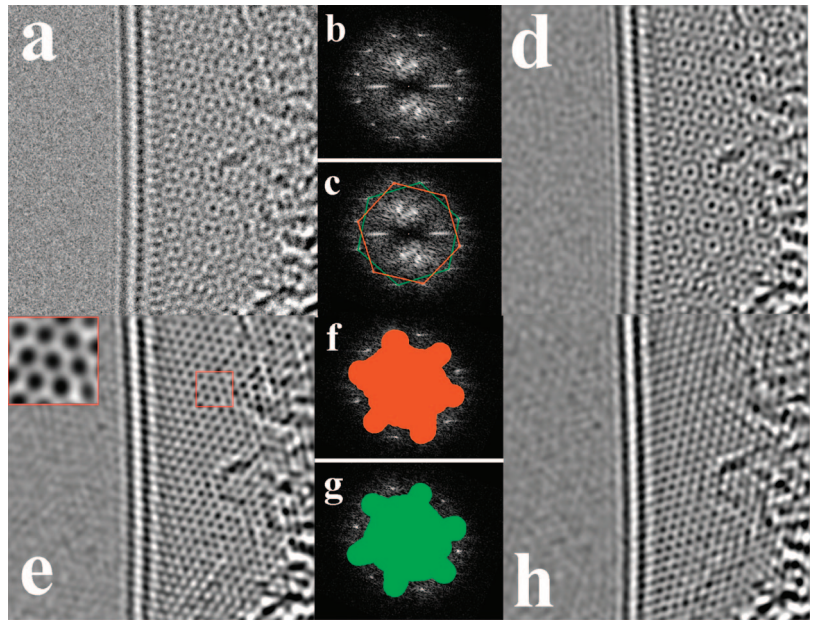


**Figure 2.** (a) Raw HRTEM image of the edge of a graphene nanosheet showing a bilayer structure with Moiré pattern. (b) Fast Fourier transform of Figure 1a showing two sets of hexagons with 30° rotation between them. (c) Red and green hexagons overlaid on the FFT to indicate the two sets of spots. (d) Reconstructed image after filtering in the frequency domain to include contributions from both sets of hexagons. (e) Reconstructed image showing the back graphene layer with one set of hexagon spots removed by filtering in the frequency domain. Inset shows a magnified section of the graphene indicated with a red box. (f) Mask used to filter in the frequency domain to obtain panel e, color region is used for the reconstructed image. (g) Mask used for the reconstructed image of the front graphene layer in panel h. (h) Reconstructed image of the front graphene layer after filtering in the frequency domain.

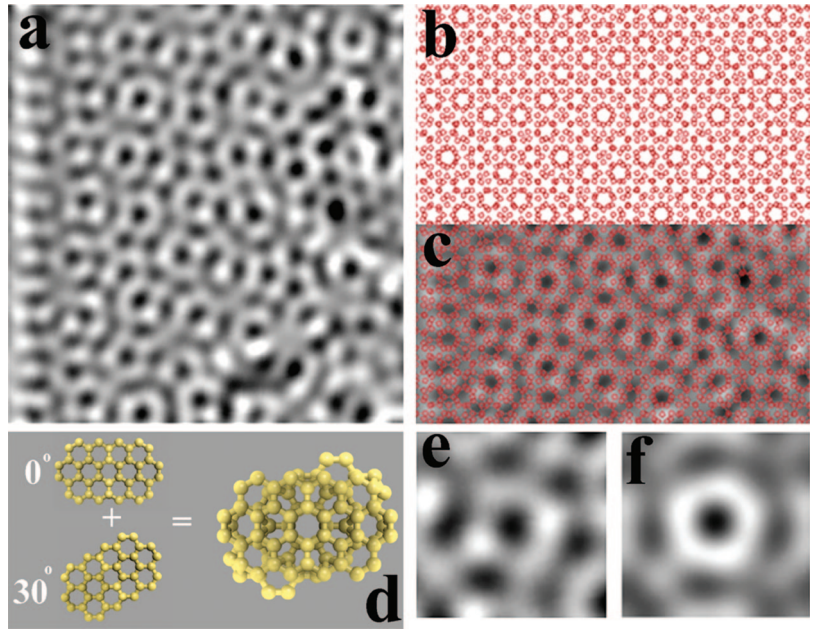


**Figure 3.** (a) HRTEM image of the Moiré pattern produced in the bilayer structure observed in Figure 2. (b) Structural representation of two graphene layers with 30° rotation. (c) Overlay of the structural representation in panel b with the HRTEM image in panel a, showing excellent agreement with the areas of contrast. (d) Schematic diagram illustrating two graphene layers with 30° rotation added together to produce a superstructure. (e) HRTEM image of the superstructure illustrated in panel d. (f) HRTEM image simulation of the superstructure illustrated in panel d and imaged in panel e showing excellent agreement.

full hexagonal lattice structure in graphene without inducing large amounts of structural damage.

Figure 1g shows a HRTEM image with aberration correction at 80 kV of a typical region of the few layer graphene nanosheets with AB Bernal stacking. The yellow area in Figure 1g shows an extra monolayer of graphene on top of the few layer graphene with no change in the observed atomic structure of the image in HRTEM. This is indicative of AB Bernal stacked multilayer graphene, where the areas of strong and weak contrast are due to the periodic overlapping of carbon atoms. Figure 1h shows a schematic illustration of the AB Bernal stacking for bilayer graphene with white spots

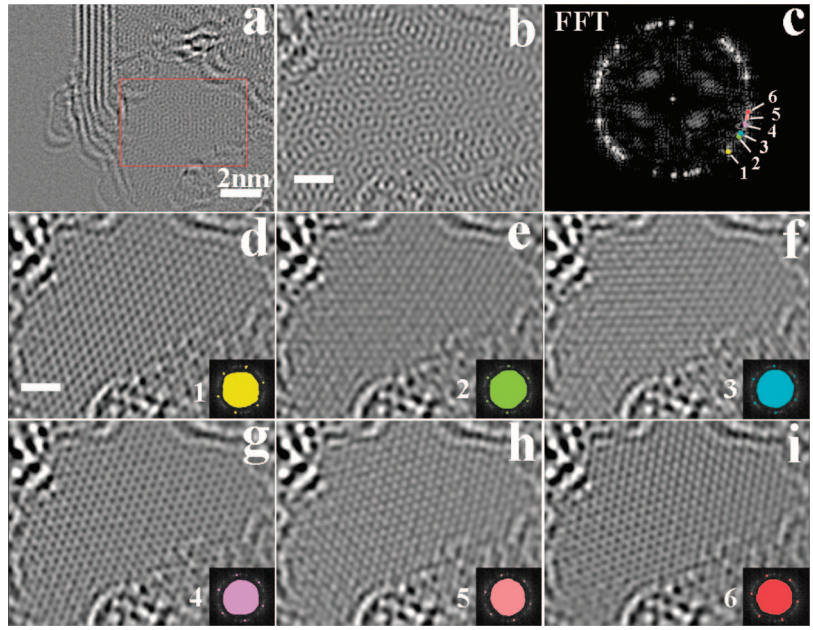


**Figure 4.** (a) HRTEM image of the edge of a few layer graphene nanosheet with at least six layers. (b) HRTEM image of the region indicated with the red box in panel a showing a complex Moiré pattern due to the relative rotations of the six layers. (c) FFT of panel b showing six sets of hexagonal spots corresponding to six different graphene layer orientations. (d−i) Reconstructed images showing the graphene layer associated with the relative set of spots indicated in panel c; inset shows the mask used.

indicating regions of overlapping carbon atoms. The red hexagons highlight the structure that gives rise to the strong contrast in the HRTEM image in Figure 1g.

We found approximately 20−30% of the few layer graphene nanosheets contained regions with observable Moiré patterns in the HRTEM images arising from rotational stacking faults. These rotational faults are most likely related to back folding of top graphene layers during the exfoliation. Intrinsic rotational stacking faults within the graphite structure may also contribute to the number of stacking faults. The Moiré patterns were examined using aberration corrected HRTEM over areas ranging between 10−200 $nm^2$. To ensure that several few layer graphene nanosheets were not probed simultaneously they were diluted in 1,2-dichloroethane and well dispersed on lacey carbon-coated TEM grids. Individual nanosheets well isolated from others were located and then examined with HRTEM.

Figure 2a shows a HRTEM image taken at the edge region of a of few layer graphene nanosheet.[18] A complex pattern is seen in Figure 2a consisting of a number of large circles, significantly different to the AB Bernal stacked few layer graphene in Figure 1g. The FFT of Figure 2a is presented in Figure 2b. A FFT of a single hexagonal graphene network produces only six spots of 0.21 nm spacing and in Figure 2b 12 spots are observed with 0.21 nm spacing. This allows a set of spots to be associated with each different orientation of graphene sheets within the layer. Figure 2c shows the corresponding sets of 6 spot hexagons for the respective front and back graphene sheets. Figure 2d shows the image reconstructed by filtering in the frequency domain to remove unwanted noise. Figure 2e shows the reconstructed image of the back graphene layer after filtering in the frequency domain using the inclusive mask shown in red in the FFT presented in Figure 2f. The hexagonal graphene network is clearly resolved in Figure 2e, with the inset showing a magnification of the small region indicated with a red box. Figure 2g shows the green inclusive mask in the FFT used to reconstruct the front graphene layer in Figure 2h. Figure 2e,h shows a rotation of 30° between the relative graphene layers that produces the Moiré pattern in Figure 2a.

Figure 3a shows a HRTEM image of the Moiré pattern for the 30° rotational stacking fault presented in Figure 2. Figure 3b shows the structural representation of two graphene layers with a 30° rotation and the resulting Moiré pattern produced. Figure 3c shows the overlay of the structural representation from Figure 3b with the HRTEM image in Figure 3a. An excellent correlation is observed between regions void of carbon atoms with regions of strong contrast in the HRTEM image, and regions containing carbon atoms with regions of weak contrast in the HRTEM image. Figure 3d is a schematic illustration of the superstructure formed by the addition of two graphene layers with 30° relative rotation. Figure 3e shows a HRTEM image of the ring shaped superstructure, and Figure 3f shows a HRTEM image simulation of the superstructure. Agreement is observed between the HRTEM image in Figure 3e and the theoretically generated image simulation in Figure 3f. This shows that Moiré patterns produced in graphene bilayers can be interpreted as the overall atomic structure produced by two graphene layers with 30° rotation, through which the electrons propagate to form a HRTEM image.

A Moiré pattern generated by only one rotational stacking fault, as examined in Figures 2 and 3, is the simplest structure to examine. We observed more complex Moiré patterns arising from areas in the graphene nanosheets containing up to six rotational stacking faults in layers. Figure 4a shows an edge with at least six graphene layers and a region containing a complex Moiré pattern, indicated with a red

box. Figure 4b shows the HRTEM image of the region containing the Moiré pattern. A FFT was taken from this region, Figure 4c, and showed six different sets of spots each attributed to a graphene layer with a distinct orientation direction. This indicates that at least six layers in this region have rotation with respect to each other. Figure 4d−i shows the reconstructed images for each layer produced by filtering in the frequency domain using the inclusive mask indicated in the inset. The hexagonal carbon network of each graphene sheet for all six orientations is resolved and the relative angles of rotation determined.

Atomic force microscopy (AFM)[1] and optical imaging[19] of graphene are regularly used to determine the number of graphene layers in sheets. While these techniques are excellent for counting layers and mapping out spatial regions with specific numbers of graphene layers, they cannot determine the presence of rotational stacking faults within these few layer structures. A single monolayer of graphene folded back onto itself will form a two layer thick graphene sheet with an arbitrary rotation between the top and bottom layers. This non-AB Bernal stacked graphene bilayer would appear almost identical to an AB Bernal stacked bilayer of graphene when analyzed using AFM or optical imaging. Selected area electron diffraction (SAED) and low energy electron diffraction (LEED)[6] are capable of measuring rotational stacking faults in few layer graphene but do not provide direct information of the spatial mapping of graphene layers with rotational stacking faults, the presence of structural defects within each layer, or the nature of the atomic structure of few layer graphene at the edges.

Aberration-corrected low-voltage HRTEM at 80 kV is an effective tool for the direct imaging of the atomic structure in graphene sheets. The interpretation of HRTEM images is relatively simple and allows rotational stacking faults to be easily characterized by analyzing in the frequency domain. These results show that the stacking in few layer graphene is not always the assumed AB Bernal stacking associated with bulk graphite. The ability to resolve the rotational stacking fault for up to six individual layers allows an accurate description of the packing structure to be determined. Knowledge of the complete packing structure of bilayer and few layer graphene is critical for determining the band structure and electronic properties. This holds great promise for correlating electronic transport studies with complete atomic structural characterization using HRTEM.

**Acknowledgment.** This work was supported in part by the Engineering and Physical Sciences Research Council (EPSRC) through the QIP IRC (No. GR/S82176/01). G.A.D.B. thanks the EPSRC for a Professorial Research Fellowship (GR/S15808/01).

## References

(1) Novoselov, K. S.; Geim, A. K.; Morozov, S. V.; Jiang, D.; Zhang, Y.; Dubonos, S. V.; Grigorieva, I. V.; Firsov, A. A. *Science* **2004**, *306*, 666–669.
(2) Novoselov, K. S.; Geim, A. K.; Morozov, S. V.; Jiang, D.; Katsnelson, M. I.; Grigorieva, I. V.; Dubonos, S. V.; Firsov, A. A. *Nature* **2005**, *438*, 197–200.
(3) Lin, Y.-M.; Avouris, P. *Nano Lett.* **2008**, *8*, 2119–2125.
(4) Latil, S.; Meunier, V.; Henrard, L. *Phys. Rev. B.* **2007**, 210402(R).
(5) Hass, J.; Varchon, F.; Millan-Otoya, J. E.; Spinkle, M.; de Heer, W. A.; Berger, C.; First, P. N.; Magaud, L.; Conrad, E. H. *Phys. Rev. Lett.* **2008**, *100*, 125504.
(6) Varchon, F.; Mallet, P.; Magaud, L.; Veuillen, J.-Y. *Phys. Rev. B* **2008**, *77*, 165415.
(7) Kobayashi, K. *Phys. Rev. B* **1996**, *53*, 5311091.
(8) Marchini, S.; Gunther, S.; Wintterlin, J. *Phys. Rev. B* **2007**, *76*, 075429.
(9) Kuwabara, M.; Clarke, D. R.; Smith, D. A. *Appl. Phys. Lett.* **1990**, *56*, 2396–2398.
(10) Coraux, J.; N'Diaye, A. T.; Busse, C.; Michely, T. *Nano Lett.* **2008**, *8*, 565–570.
(11) Ong, T. S.; Yang, H. *Carbon* **2000**, *38*, 2077–2085.
(12) Krasheninnikov, A. V.; Banhart, F. *Nat. Mater.* **2007**, *6*, 723–733.
(13) Meyer, J. C.; Kisielowski, C.; Erni, R.; Rossell, M. D.; Crommie, M. F.; Zettl, A. *Nano Lett.* **2008**, *8*, 3582–3586.
(14) Hashimoto, A.; Suenaga, K.; Gloter, A.; Urita, K.; Iijima, S. *Nature* **2004**, *430*, 870–873.
(15) Suenaga, K.; Wakabayashi, H.; Koshino, M.; Sato, Y.; Urita, K.; Iijima, S. *Nature* **2007**, *2*, 358–360.
(16) Zhu, H.; Suenaga, K.; Hashimoto, A.; Urita, K.; Iijima, S. *Chem. Phys. Lett.* **2005**, *412*, 116–120.
(17) Sato, Y.; Suenaga, K.; Okubo, S.; Okazaki, T.; Iijima, S. *Nano Lett.* **2007**, *7*, 3704–3708.
(18) Meyer, J. C.; Geim, A. K.; Katsnelson, M. I.; Novoselov, K. S.; Booth, T. J.; Roth, S. *Nature* **2007**, *446*, 60–63.
(19) Jung, I.; Pelton, M.; Piner, R.; Dikin, D. A.; Stankovich, S.; Watcharotone, S.; Hausner, M.; Ruoff, R. S. *Nano Lett.* **2007**, *7*, 3569–3575.

NL8025949